

THE 4TH INTERNATIONAL CONFERENCE ON ALUMINUM ALLOYS

ELEVATED TEMPERATURE CRACK GROWTH OF ALUMINUM ALLOY 2519

B.C. Hamilton and A. Saxena
Georgia Institute of Technology
School of Materials Science and Engineering
Atlanta, GA 30332-0245, USA

Abstract

Aluminum 2519-T87, an aluminum-copper alloy containing 5.3%-6.4% copper, was developed as an improvement to aluminum 2219. This alloy is precipitation hardened by rapid quenching from the single phase regime followed by solution heat treatment to form θ' precipitates. Because 2519-T87 displays excellent retention of mechanical properties over a wide temperature range, it is a candidate alloy for future applications in high speed aircraft. Creep crack growth is an important consideration in this application. Utilizing compact type specimens, creep crack growth behavior of 2519-T87 has been characterized, and the appropriate crack tip parameter (K or C) which correlates better with the creep crack growth rate has been identified.

Introduction

Aluminum 2519-T87 is a precipitation hardened aluminum-copper alloy that contains 5.3%-6.4% copper. Fabrication of the alloy begins by heating to approximately 540°C. At this temperature, only the single α phase exists, and all copper dissolves in the aluminum, forming a solid solution. The alloy is then rapidly quenched from the single phase regime to room temperature. The solid solubility of copper sharply declines at the lower temperature, but the rapid quench suppresses the formation of any copper precipitates. Thus, the solid solution becomes supersaturated with copper, despite a thermodynamic driving force to form CuAl_2 , θ precipitates.⁽¹⁾ Following the quench, the solution is heat treated and aged to induce precipitate nucleation. Most important to the enhancement of mechanical properties, such as the yield strength, are the θ' precipitates, also CuAl_2 stoichiometrically. These particles are partially coherent in the matrix and serve as effective barriers to dislocation motion due to the strain energy and interfacial energy associated with the second phase. Though metastable, θ' precipitates can exist in the microstructure at room temperature, unlike the θ'' precipitates and GP zones which are too unstable at these temperatures. The equilibrium θ phase will also be present in the final microstructure of the alloy, but does not offer as effective strengthening characteristics as the θ' phase. Since the precipitate is completely incoherent in the matrix, the θ phase does not have an associated strain energy field to help impede dislocation motion.⁽¹⁾

Due to the transitory behavior of the precipitates in an aluminum-copper alloy, microstructural stability of 2519-T87 is an important issue for use in structural applications designed for extended lifetimes, particularly at elevated temperatures. The alloy, however, has been shown to retain

mechanical properties over a wide temperature range. Aluminum 2519-T87 was developed as an improvement to aluminum 2219, which has been used in such applications as ballistic armor on military vehicles.⁽²⁾ 2519-T87 provides superior mechanical properties to 2219, such as yield strength which is 15% greater (400MPa as opposed to 352MPa).⁽²⁾ Due to its lightweight and excellent retention of mechanical properties at elevated temperatures, 2519-T87 is a candidate alloy for future applications in high speed aircraft. Creep deformation and creep crack growth are important considerations for this application. In this paper, the creep crack growth behavior of 2519-T87 is characterized at 135°C (275°F), and the appropriate crack tip parameter which correlates with the creep crack growth rate is explored.

The field of time dependent fracture mechanics (TDFM) attempts to model the influence of creep on crack growth in metals by identifying the appropriate crack tip parameter which correlates with the creep crack growth rate. In general, metals undergoing creep deformation and creep crack growth are classified into two categories, creep brittle and creep ductile. In creep ductile materials, the rate of accumulation of creep strain ahead of the crack tip is much greater than the crack growth rate. Thus, the crack can be considered to be nearly stationary within a field of expanding creep zone; therefore, the stationary crack tip parameters, such as C^* or C_t ,^(3,4) characterize the creep crack growth behavior in these materials. In creep brittle materials, the crack growth rate and the rate of creep strain accumulation are comparable, and therefore, the crack tip stress fields are significantly influenced by the growing crack. Under special circumstances, the stresses ahead of the crack tip in creep brittle materials may be characterized by the time-independent parameters, such as the stress intensity parameter, K , or the J-Integral.^(5,6) In the following sections, the experimental procedure, the creep deformation behavior, and the crack growth behavior are first described, and the results are subsequently discussed.

Experimental Procedures

The test material was received in the plate form, and several creep deformation and creep crack growth tests were performed at 135°C (275°F) to characterize the creep and creep crack growth behavior of aluminum 2519. For creep deformation testing, twelve miniature specimens were

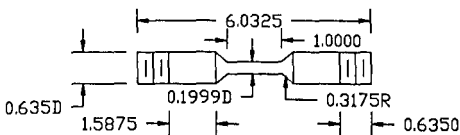


Figure 1-Creep deformation specimen geometry (Unit: cm)

machined from the plate material. The selected geometry and size is shown in Figure 1. The miniature size was chosen because the amount of plate material was limited. Creep deformation tests were performed with dead-weight loaded creep machines. In some cases the load was applied directly on the specimens. Creep deflection was measured with a direct voltage displacement transducer (DVDT)

based extensometer, and the gage output was recorded using a Bitlogger recorder. The Bitlogger is a digital data acquisition device in which the frequency of data acquisition can be preset.

Four CT type specimens were machined from the plate material in the L-T orientation for creep crack growth testing. The specimens were 5.080cm wide, measured from the load line, and

2.210cm thick. The initial machined notch depth was 1.905cm from the load-line of the specimen. The four specimens were fatigue precracked using a servohydraulic system to an initial crack length of 2.159cm. The final 0.0635cm of precrack extension was obtained at a ΔK level of $4.4\text{MPa}\sqrt{\text{m}}$, well below the test K-levels. Following precracking, the specimens were side grooved 10% of the thickness on each side of the crack plane. The creep crack growth tests were performed using dead-weight lever type creep machines.

A heater tape was wrapped around the specimens to heat them to the test temperature. To insure a uniform temperature in the specimen, the heater tape was not directly applied to the sample. Instead, a small cage from a wire mesh was configured around the specimen, and the heater tape was wrapped on the cage. The assembly was then wrapped with Kaowool for insulation. The overall setup resembled a small furnace and performed similarly. The load-line deflection was measured continuously with time using a

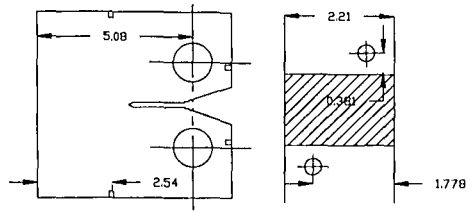


Figure 2-Potential lead locations (Unit: cm)

DVDT extensometer attached to the knife blades which were inserted into the notch.^(7,8) The crack length was measured through the DC potential drop method with lead locations configured to relate output voltage to crack size using the Johnson's formula,⁽⁹⁾ refer to Figure 2. In addition to the DC potential method, crack extension was also determined by visual measurement and by compliance change. Signals from both the DVDT and the potential drop were recorded on a strip chart recorder for continuous monitoring

Table I-Creep Deformation Tests

Specimen #	Stress Level (MPa)	Time to failure(hr)
CD-1	310	2850
CD-2	352	16 min
CD-4	317	>45
CD-5	324	>60

throughout the test duration. The crack growth rates were calculated utilizing the secant (point to point) method.⁽⁸⁾

Results and Discussion

Four creep deformation tests have been completed for which the results are summarized in Table I. Though creep deformation does occur, the percent strain to fracture varies from only 1.2% to 2.0%, which is consistent with the creep brittle behavior of the material. Creep strain versus time data is presented in Figure 3 for two different stress levels, 317MPa (CD-4) and 324MPa (CD-5). For both curves the extent of primary creep deformation is small with respect to the failure time (less than 1%), but as a fraction of the strain to fracture, primary creep contributes significantly to the total deformation. Also evident are the steady-state and tertiary creep regimes. In Figure 4, the log of the steady state creep rate is plotted against the log of the applied stress. This

$$\frac{de_{ss}}{dt} = A\sigma^n \quad (1)$$

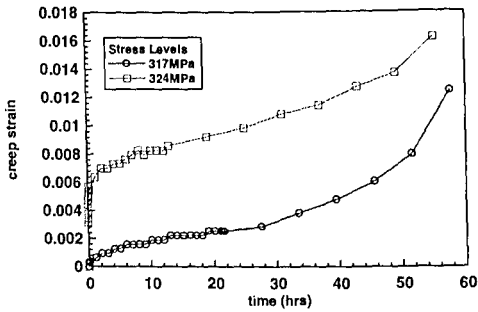


Figure 3-Creep strain as a function of time for two stress levels

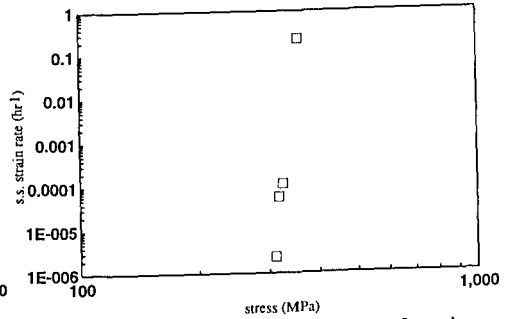


Figure 4-Steady state creep rate as a function of the applied stress

plotting technique permits the calculation of the steady state creep coefficient and exponent as presented in equation (1). A regression line fitted through the four data points yields $n=82.8$ and $A=10^{-142.3}$, which may appear extreme, but are not inconsistent with data on other high temperature aluminum alloys. Considering the steep slope of the regression line, these constants simply demonstrate that the steady-state creep behavior of aluminum 2519 is highly sensitive to the applied stress.

A summary of conditions for the creep crack growth tests is presented in Table II. Aluminum

Table II-Creep crack growth tests

Specimen #	K-level (MPa√m)	Initial Crack Length (cm)	Final Length Potential (cm)	Final Length Comp. (cm)	Failure time (hrs)
BCH-4	16.51	2.253	2.642	3.150	354
BCH-5	18.73	2.256	2.845	3.251	31
BCH-6	18.73	2.250	2.718	2.718	104
BCH-7	17.60	2.258	2.769	2.642	stopped

2519 displayed little creep deformation and creep crack extension. The three specimens which failed experienced rapid, brittle fracture after a certain amount of creep crack extension. The visual measurement of final crack lengths, therefore, proved to be a difficult task since the fast fracture surface could not be distinguished from the end of the creep cracks. Crack length data for BCH-7 as a function of time is presented in Figure 5 and also presented are the final crack lengths measured by the three methods. Specimen BCH-7 was utilized to visually measure a final crack length that could be compared to the other two methods for determining crack extension, DC potential drop and compliance change.⁽¹⁰⁾ BCH-7 was stopped after 150 hours and then fatigued using a servohydraulic machine. The fatigue surface could be discerned from the creep crack surface and served as a bench mark for accurately measuring creep crack extension. The total crack lengths calculated through potential drop and compliance change both differ by less than 3% from the visually determined length and less than 5% from each other. Certainly, these results support the validity of compliance change as a technique for determining crack extension. Not all other data, however, support this conclusion as strongly. For example, the final crack

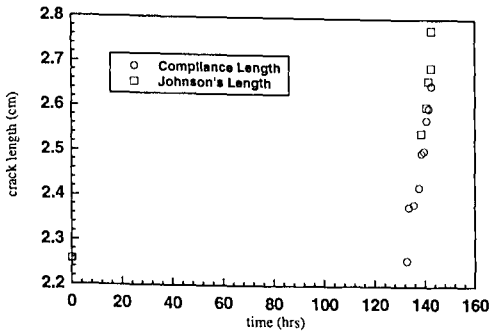


Figure 5-Crack length comparison for BCH-7

lengths of BCH-4 determined by the potential method and compliance change differ by nearly 20% (3.150cm by compliance and 2.642cm by potential drop). This discrepancy can be explained by considering the assumptions surrounding the compliance technique. Compliance change assumes elastic conditions prevail and that any changes in deflection are elastic. Contributions to deflection from creep deformation are ignored. This assumption is not unfounded since aluminum 2519 exhibits creep resistant behavior, and the majority of deflection that occurs is elastic, particularly in the fast fracture regime of the test; however, for tests,

such as BCH-4, which are performed at lower K-levels, a definite contribution to deflection from creep exists and influences the comparison between the potential drop method and compliance change. Both techniques, however, were utilized to measure crack lengths and calculate K and C_I values.

The stress intensity factor, K, is easily calculated from the crack lengths using equation (2),

$$K = \frac{P f\left(\frac{a}{W}\right)}{B_N W^{\frac{1}{2}}} \quad (2)$$

where P is the load, W is the specimen width, f(a/W) is a geometric factor, and B_N is the net specimen thickness. The net specimen thickness corrects for side grooving of the CT samples and is defined as B_N = √B_{sg}B, where B is the original specimen thickness, and B_{sg} is the specimen thickness in the side groove plane. Figure 6 shows the correlation between K and the creep crack growth rate using the potential drop method to calculate the crack length. The data from the four tests correlates well and suggests that the stress intensity factor is the appropriate fracture parameter that characterizes the crack tip stress amplitude. This result is consistent with the behavior of a creep brittle material.^(11,12) Certainly, aluminum 2519 displayed limited creep deformation; therefore, the accumulation of creep strain was confined to a small zone at the crack tip (small scale creep), while the majority of the stresses ahead of the crack tip were K controlled. The crack growth rate surpassed the creep strain accumulation rate, giving the correlation of crack growth rate with K. With this data, the following relationship between K and the crack growth rate can be developed.⁽¹¹⁾

$$\frac{da}{dt} = A' K^q \quad (3)$$

where A' and q are regression constants. Figure 7 shows the correlation between K and the creep crack growth rate using the compliance change to calculate the crack length. Again, the data from

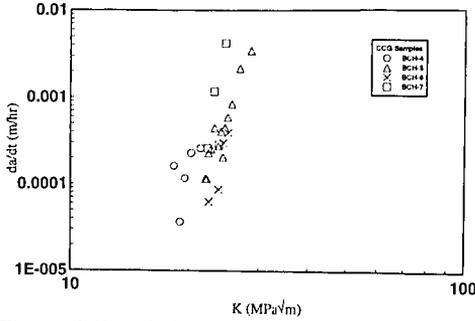


Figure 6-Correlation with K using DC potential method

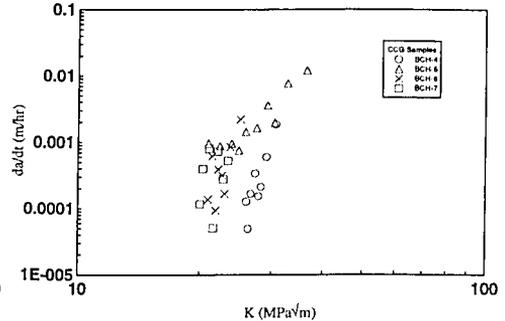


Figure 7-Correlation with K using compliance change

the four tests correlate well and even correlate with the results from the potential method. The data from BCH-4, however, exhibits more scatter under the compliance method than is ideally desired. The reason for this scatter lies in the assumption of the compliance method that all deflection is elastic. BCH-4 was performed at the lowest K-level of the four tests and accumulated the most creep deformation; therefore, the deflection data from BCH-4 contained a larger creep component than any of the other tests, creating the scatter in the correlation plot of K and the creep crack growth rate in Figure 7.

Small scale creep conditions predominate in the CT specimens at 135°C. The following equation is used to calculate C_t values for small scale creep:^(8,12)

$$(C_t)_{ssc} = \frac{P\dot{V}_c}{B_N W} (F'/F) \quad (4)$$

where

$$F = \left(\frac{K}{P}\right) B_N W^{\frac{1}{2}} \quad F' = \frac{dF}{d\left(\frac{a}{W}\right)} \quad (5)$$

\dot{V}_c is the creep deflection rate, which is determined by partitioning the entire deflection rate into contributions from creep, elastic deformation (\dot{V}_e), and plastic deformation (\dot{V}_p):^(8,12)

$$\dot{V} = \dot{V}_c + \dot{V}_e + \dot{V}_p \quad (6)$$

$$\dot{V}_c = \dot{V} - \frac{d\dot{B}}{P} \left[\frac{2K^2}{E} + (m+1)J_p \right] \quad (7)$$

The plastic contribution is taken as negligible. Figure 8 plots the normalized creep deflection rate

as a function of the crack extension (determined from potential drop method) and demonstrates

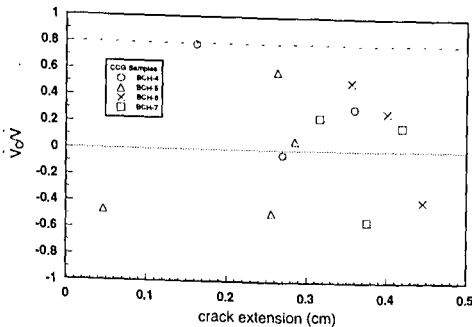


Figure 8-Change in normalized creep deflection rate with crack extension

that for all creep crack growth tests, the creep contribution is less than 80% the total deflection rate. Also, as the crack length increases, the creep contribution declines as the fast, elastic fracture regime is approached. Equation (6) is more accurate when the creep deflection rate dominates the total deflection rate. Thus, for creep contributions less than 80% of the total deflection,⁽⁸⁾ the equation lacks precision as the elastic term becomes significant, and partitioning the total deflection rate loses validity. In fact, when the elastic contribution dominates, the equation can yield negative creep deflection rates, as seen in Figure 8. Another reason for the

negative rates is that the total deflection rate is experimentally measured and will contain some experimental error that could bring about negative creep deflection rates. The negative creep deflection rates will lead to negative C_i values, which are simply meaningless; therefore, no plots of creep crack growth rate and C_i were generated. The lack of correlation with C_i is consistent with creep brittle behavior. Also, because plasticity was negligible and because extensive creep conditions did not prevail in the specimens, correlation of the data with J and C^* was not attempted. The stress intensity factor, K , displays good correlation with the creep crack growth rate and is the appropriate crack tip parameter for aluminum 2519-T87 at this test temperature.

Conclusions

- 1) At 135°C, creep crack growth rates correlate with the stress intensity factor K , not C_i . Negative C_i values were calculated, reflecting the significant contribution of the elastic deflection rate to the total deflection rate and the lack of creep deformation in the specimens.
- 2) Aluminum 2519-T87 behaves in a creep brittle fashion at 135°C. Under these conditions, the stationary crack tip parameters, such as C_i or C^* , from TDFM, are no longer applicable and fail to characterize the amplitude of the crack tip stress. The stress fields ahead of the crack tip remain K -controlled for creep brittle materials.
- 3) Compliance change is a viable method for determining crack growth rates in creep brittle materials. The compliance method assumes that all changes in deflection are elastic. This assumption will create some error in crack length calculations; however, the creep resistant nature of 2519 at 135°C justifies this assumption.

Acknowledgements

The authors would like to thank the NASA Langley Research Center for their support of this work. We would especially like to thank Dr. Robert S. Piascik at NASA Langley for his direction and input.

References

- 1 **Porter, D.A. and Easterling, K.E.**, Phase Transformations in Metals and Alloys (London, Chapman and Hall, 1981) pp. 291-302
- 2 **Chase, M., Kackley, N., and Bethoney, W.** "Engineering and Ballistic Properties of a Newly Developed 2XXX Series Aluminum Alloy Armor"
- 3 **Landes, J.D. and Begley, J.A.** in "Mechanics of Crack Growth" *ASTM STP 590* American Society for Testing and Materials (1976) pp. 128-148
- 4 **Saxena, A.** in *ASTM STP 905* (Eds. J. H. Underwood et al.) (1986) pp. 185-201
- 5 **Hutchinson, J.W.** *J. Mech. Phys. Solids* **16** (1968) pp. 13-31
- 6 **Rice, J.R. and Rosengren, G.F.** *J. Mech. Phys. Solids* **16** (1968) pp. 13-31
- 7 **Jones, K.A.**, Master's Thesis, Georgia Institute of Technology, Atlanta, GA (1993)
- 8 "Standard Test Method for Measurement of Creep Crack Growth Rates in Metals" ASTM E1457-92
- 9 **Johnson, H.H.** *Mater. Res. Standards* **5** (9) (1965) pp. 442-445
- 10 "Standard Test Method for J_{IC} , A Measure of Fracture Toughness" ASTM E813-89
- 11 **Bensussan, P.L. and Pelloux, R.M.** "Creep Crack Growth in 2219-T851 Aluminum Alloy: Applicability of Fracture Mechanics Concepts", Vol. 3 *ICF6* (1984) pp. 2167-2179
- 12 **Dogan, B., Saxena, A., and Schwalbe, K.H.** *Materials at High Temperatures* **10** (1992) pp. 138-143
- 13 **Saxena, A.** *Materials at High Temperatures* **10** (1992) pp. 79-91